Extracting target-specific characteristics from sonar measurements: Preliminary results using the matrix pencil method

Prepared by:
Raviraj S. Adve
Dept. of Electrical and Computer Engineering
University of Toronto
10 King's College Road
Toronto, Canada, M5S 3G4

Contract Scientific Authority
Vincent Myers
Defence Scientist
1-902-426-3100 ext 167

PWGSC Contract Number: W7707-135620

Contract Report

DRDC-RDDC-2016-C106

March 2016

Extracting Target-Specific Characteristics from Sonar Measurements : Preliminary Results using the Matrix Pencil Method

Raviraj S. Adve

Dept. of Electrical and Computer Engineering
University of Toronto
10 King's College Road
Toronto, Ontario, M5S 3G4, Canada

rsadve@comm.utoronto.ca

Progress Report

March 31, 2016

Abstract

In underwater sonar systems, identifying targets from their signatures is an important, but, yet, open problem. In an earlier document, we had proposed to extract the fundamental modes of a target based on the Matrix Pencil and Cauchy approaches. This report presents the results of a preliminary analysis of PONDEX data sets provided by Defense Research and Development Canada (DRDC) Atlantic. The data set includes the sonar returns from a variety of targets and target-like objects. As our results will show, in our *preliminary* analysis the Matrix Pencil approach is able to distinguish between two very different kinds of targets. We also discuss more cautionary results using comparisons of similar objects in different settings. However, since this report is written after only a very preliminary investigation, we conclude that there is some promise in the notion of target discrimination and identification using the Matrix Pencil approach.

1 Introduction

An underwater synthetic aperture sonar (SAS) system provides high-resolution images of the sea-bed allowing for the detection of man-made objects such as mines, shells and debris. The goal of this project is to enhance discrimination between the objects detected, i.e., to improve the classification and identification of objects detected. To achieve this goal, it is essential to obtain class or object specific characteristics that, then, allow for this discrimination. Specifically, this project furthers this goal by investigating two techniques that treat the target as an input-output system extract the fundamental modes of the system. In previous work, in noise-radar systems detecting concealed weapons, we showed that these approaches can potentially discriminate between different types of weapons [1].

The two suggested techniques are the Matrix Pencil algorithm [2,3] and the Cauchy method [4]. They each treat the target identification problem as estimating the fundamental modes of a system. The two techniques, using time and frequency domain data respectively, are forms of model-based parameter estimation. Specifically, the Matrix Pencil approach models the (sampled) time domain signal as a linear sum of complex exponentials; the goal is to find the parameters of the linear sum - the exponents, that are related to the modes, and the amplitudes (if required). While a sum-of-exponentials is a well-established model, Matrix Pencil differs from other techniques in not requiring any statistical information. A single snapshot of collected data is adequate to execute the algorithm. The approach has been used in multiple applications such as indoor localization [5] and compensation for mutual coupling in adaptive processing [6].

The Cauchy method, on the other hand, models the frequency domain information as the ratio of two complex polynomials. As with the Matrix Pencil method, the goal is to find the coefficients of the polynomials which can then be factored to find the poles and zeros of the system at hand. Importantly, like the Matrix Pencil approach described above, a single snapshot of frequency domain data is adequate to execute the algorithm. The algorithm uses the Total Least Squared approach to minimize the impact of noise and estimate the orders of the polynomials involved.

The plan for this and next year is to test the use of the Matrix Pencil and Cauchy methods in distinguishing, using the modes, targets of different kinds. The two-stage plan is to first finish a proof-of-concept analysis using the PONDEX data [7] made available by DRDC in March 2016. Depending on the results of using this data set, and whatever SAS data is available, the second stage will build on the lessons learned to investigate target identification and discrimination using high-frequency SAS measurements.

This report presents the preliminary results investigating the use of the Matrix Pencil in the context of the PONDEX data sets. Specifically, we analyze a subset of the targets: the aluminium pipe, the aluminium UXO shell placed on a flat sand/water interface (the "proud" setting) at distances of 5m and 10m from the sonar, the same UXO shell buried at 5m and a real UXO shell (proud at 10m). For completeness, we begin with a review of the Matrix Pencil algorithm.

2 Matrix Pencil

In the Matrix Pencil approach, the time domain signal, here $x(t)$, is modeled as a sum of complex exponentials:

$$x(t) = \sum_{m=1}^{M} A_m e^{\zeta_m t}; \qquad \zeta_m = \alpha_m + j\beta_m, \tag{1}$$

where $\zeta_m, m = 1, \ldots, M$ represent the complex poles of the system. Let $z_m = e^{\zeta_m \Delta t}$, where Δt is the sampling period. Then

$$x[k] = x(k\Delta t) = \sum_{m=1}^{M} A_m z_m^k; \qquad k = 0, 1, \ldots, K-1. \tag{2}$$

The system is, therefore, identified by estimating M, the number of poles and $z_m, m = 1, \ldots, M$. Using the estimate of the poles, the amplitudes of the individual components, $A_m, m = 1, \ldots, M$ can then be estimated.

The Matrix Pencil approach to estimate these parameters is as follows: form the $(K-L)\times(L+1)$

matrix $\mathbf{X}$ defined as the

$$\mathbf{X} = \begin{bmatrix} x[0] & x[]1 & \cdots & x[L-1] & x[L] \\ x[1] & x[2] & \cdots & x[L] & x[L+1] \\ \vdots & \vdots & \ddots & \vdots & \vdots \\ x[K-L-1] & x[K-L] & \cdots & x[K-2] & x[K-1] \end{bmatrix}, \tag{3}$$

where L is called the pencil parameter. Define two $(N-L) \times L$ matrices $\mathbf{X_0}$ and $\mathbf{X_1}$ as the first L and last L columns of $\mathbf{X}$, i.e. in MATLAB notation

$$\mathbf{X_0} = \mathbf{X}(:, 1:L) \tag{4}$$
$$\mathbf{X_1} = \mathbf{X}(:, 2:L+1). \tag{5}$$

These two matrices can be written as

$$\mathbf{X_0} = \mathbf{Z}_1 \mathbf{A} \mathbf{Z}_2, \tag{6}$$
$$\mathbf{X_1} = \mathbf{Z}_1 \mathbf{A} \mathbf{Z}_0 \mathbf{Z}_2, \tag{7}$$

where,

$$\mathbf{Z}_1 = \begin{bmatrix} 1 & \cdots & 1 \\ z_1 & \cdots & z_M \\ \vdots & \ddots & \vdots \\ z_1^{(K-L-1)} & \cdots & z_M^{(K-L-1)} \end{bmatrix}_{(N-L)\times M} \tag{8}$$

$$\mathbf{Z}_2 = \begin{bmatrix} 1 & z_1 & \cdots & z_1^{L-1} \\ 1 & z_2 d & \cdots & z_2^{L-1} \\ \vdots & \vdots & \ddots & \vdots \\ 1 & z_M & \cdots & z_M^{L-1} \end{bmatrix}_{M\times L}, \tag{9}$$

$$\mathbf{Z}_0 = \operatorname{diag}\begin{bmatrix} z_1 & z_2 & \cdots & z_M \end{bmatrix}, \tag{10}$$

$$\mathbf{A} = \operatorname{diag}\begin{bmatrix} A_1 & A_2 & \cdots & A_M \end{bmatrix}. \tag{11}$$

Based on Eqn. (7), our goal is to estimate the entries of the matrix $\mathbf{Z}_0$.

Consider the following formulation, called a matrix pencil (and hence the name of the algorithm):

$$\mathbf{X_1} - \lambda \mathbf{X_0} = \mathbf{Z}_1 \mathbf{A} \left[\mathbf{Z}_0 - \lambda \mathbf{I}\right] \mathbf{Z_2}. \tag{12}$$

Choosing $\lambda = z_m$, for some m, reduces the rank of the pencil by one. The estimates for z_m are, therefore, the *generalized eigenvalues* of the matrix pair $[\mathbf{X}_1, \mathbf{X}_0]$. This approach allows for unambiguous estimation of the poles if

$$M \leq L \leq K - M. \tag{13}$$

The amplitudes $A_m, m = 1, \ldots, M$ can then be obtained by a least squares estimate [3].

2.1 TLS Matrix Pencil

The approach described above has been shown to be sensitive to the presence of thermal noise in the received signal. A more robust approach is the Total Least Squares approach [3].

Define the singular value decomposition (SVD) of the matrix $\mathbf{X}$ as

$$\mathbf{X} = \mathbf{U}\mathbf{\Sigma}\mathbf{V}^H, \tag{14}$$

where ^{H} represents the Hermitian or conjugate transpose of a matrix. In the absence of thermal noise, assuming the constraint in Eqn. (13) is met, exactly M of the singular values are non-zero. In the presence of thermal noise, estimating M becomes an issue of estimating the number of statistically significant singular values in noise. There is unfortunately, no best scheme to do this and the accuracy of the estimate is a function of the SNR [8].

Having estimated M, the data matrix $\mathbf{X}$ is filtered by dropping all but the largest M singular values. Defining $\mathbf{\Sigma}'$ as the diagonal matrix with the M largest singular values and $\mathbf{U}'$ and $\mathbf{V}'$ as the corresponding matrices of left and right singular vectors. Let $\mathbf{X}' = \mathbf{U}'\mathbf{\Sigma}'\mathbf{V}'^H$. The total least squares Matrix Pencil then follows the same approach as described above, but with matrices $\mathbf{X}_0$ and $\mathbf{X}_1$ formed from the filtered data matrix $\mathbf{X}'$.

An alternative approach that achieves the same purpose is to define $\mathbf{V}_0$ and $\mathbf{V}_1$ as the first and second L rows of the matrix $\mathbf{V}$, i.e., in MATLAB notation again,

$$\mathbf{V_0} = \mathbf{V}(1:L, 1:M) \tag{15}$$

$$\mathbf{V_1} = \mathbf{V}(2:L+1, 1:M). \tag{16}$$

The M poles are then the generalized eigenvalues of the matrix pair $[\mathbf{V}_0, \mathbf{V}_1]$.

3 Numerical Results

3.1 The PONDEX Data Set and Pre-processing

The PONDEX data set, provided by DRDC, is described in [7] and in an explanation file that accompanies the data. The data comprises measurements of various targets, each in 9 different orientations, ranges. In some cases the same target is or is not buried. The transmitted signal appears to be a linear FM covering the frequency range from 1 kHz to 30 kHz, i.e., this is relatively low-frequency data. Furthermore, each of the 9 measurements, for the same target orientation and range, includes measurements from 2000 time samples for each of 1600 cross-range positions. The sampling rate appears to be 10^5 samples per second, i.e., $\Delta t = 1 \times 10^{-5}$. Of these, the center position, position 801, has the target closest to the sonar. The time samples associated with this position is used for further investigation. Importantly, *we do not attempt to deconvolve the transmitted signal from the measurements.*

Figure 1 plots the measured signal at the center position for the aluminium UXO shell proud at 10m. The figure shows that most of the measured signal is essentially zero before the transmitted signal impinges on the target and again after a transient has died down. Furthermore, the signal has a waxing phase (modes would have positive values of α_m) and a waning phase (modes would have negative values of α_m). This presents a problem for the Matrix Pencil approach which treats the modes as unknown constants to be estimated.

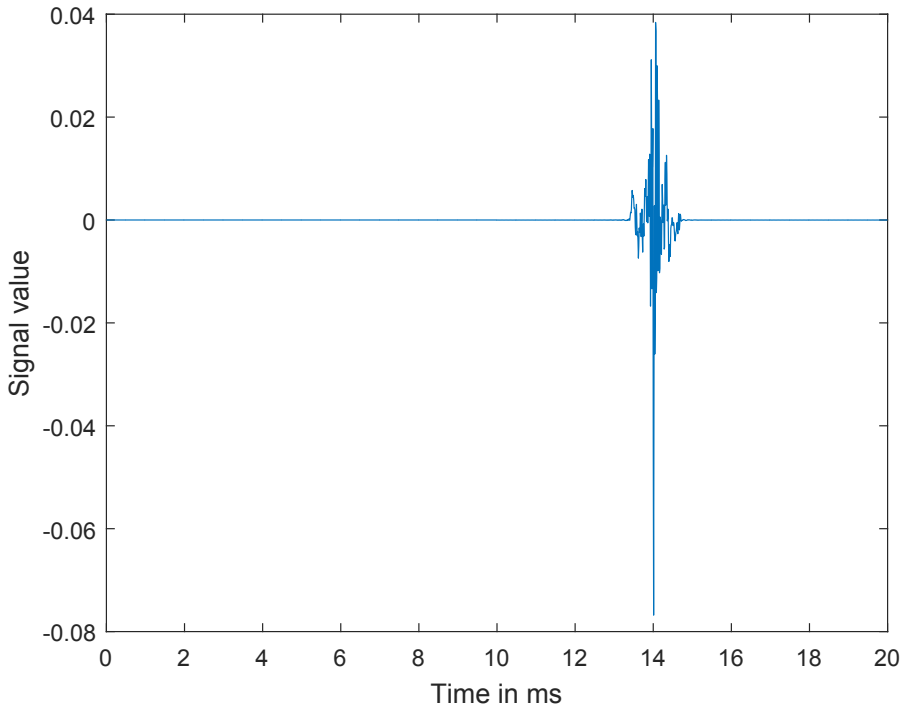

Figure 1: Complete measured signal at the center position. Aluminium UXO shell, proud at 10m.

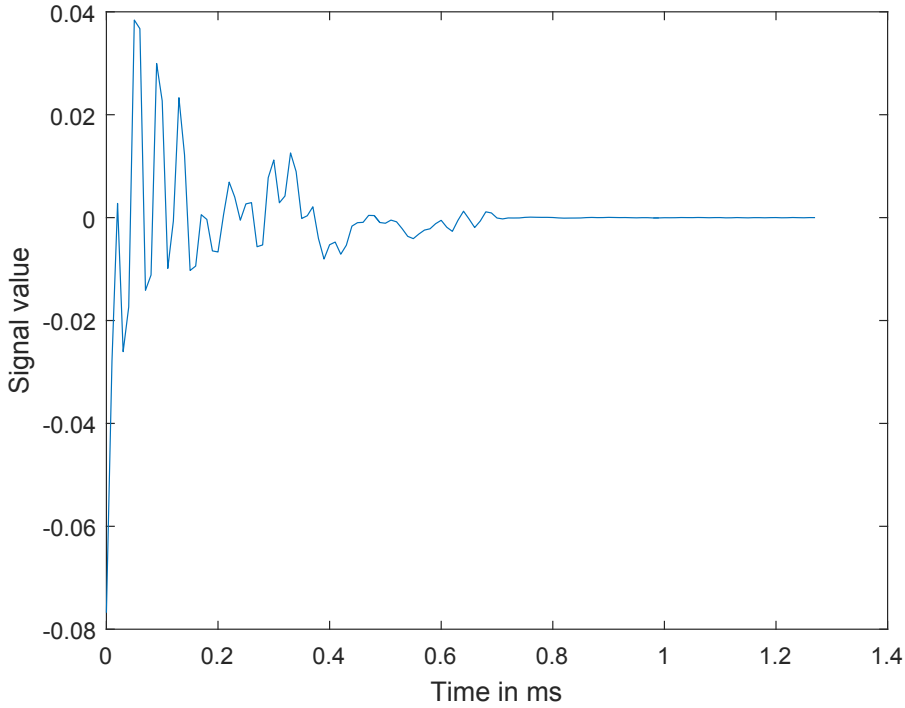

Figure 2: Segment of measured signal use for analysis. Aluminium UXO shell, proud at 10m.

To bypass this problem, we use a segment of the signal that begins at the maximum absolute value of the signal. Figure 2 illustrates the segment of the signal used. In this report, all the signals used "begin" at the point where they take their maximum absolute value; the segment used covers 128 samples, i.e., $K = 128$. Since the Matrix Pencil approach requires that $M < L$, we chose $L \simeq K/2 = K/2 - 1 = 63$.

3.2 Algorithm Implementation and Choice of Number of Modes (M)

In this reporting period, we implemented the simplest form of the TLS Matrix Pencil, leaving aside the estimation of the number of modes, M. Both the parameter, L and the number of modes, M, are user-defined parameters. One reason for this implementation is that, so far, we do not know how many modes with small amplitudes are really required for the discrimination process. To illustrate this, Fig. 3 plots the singular values, in descending order, of the data matrix $\mathbf{X}$ for the case of the aluminium UXO target proud at 10m. Using the traditional approach of using the "knee of the curve", the figure suggests that the matching the data requires about 40 modes, i.e., $M \simeq 40$. This seems like a remarkably large number for a smooth target like the aluminium UXO shell and is a cause for concern.

Figure 4 illustrates the problem - the figure plots the amplitude of the individual modes (sorted). As is clear from the figure, the dynamic range of the modes identified is as much as 60dB. However, at this stage, it is unclear as to whether it is the dominant modes, with the large amplitudes, that help discriminate between targets or the weaker modes that may capture the behaviour of special characteristics of the target.

Figure 5 illustrates the efficacy of the Matrix Pencil approach, albeit with a large value of $M = 40$. The original data is the measured data shown in Fig. 2. The reconstructed data is the signal reconstructed using Eqn. (2) after obtaining the modes and mode amplitudes as described above. As is clear, the two are indistinguishable and the algorithm does model the measured signal very well. This plot suggests that the small amplitude modes are useful to describe the small variations in the measured signal.

This observation is reinforced by Figs. 6 and 7. The two figures plot the pre-processed signal for the aluminium pipe with two different choices of $M = 16$ and $M = 40$. As is clear from the figures, the case of $M = 16$ does capture the essential behaviour of the measured signals, but it is the $M = 40$ case that captures the fine-grained details.

In our next set of results, for ease of illustration, we choose $M = 16$. We will compare the modes obtained for the various targets and discuss both promising and cautionary results.

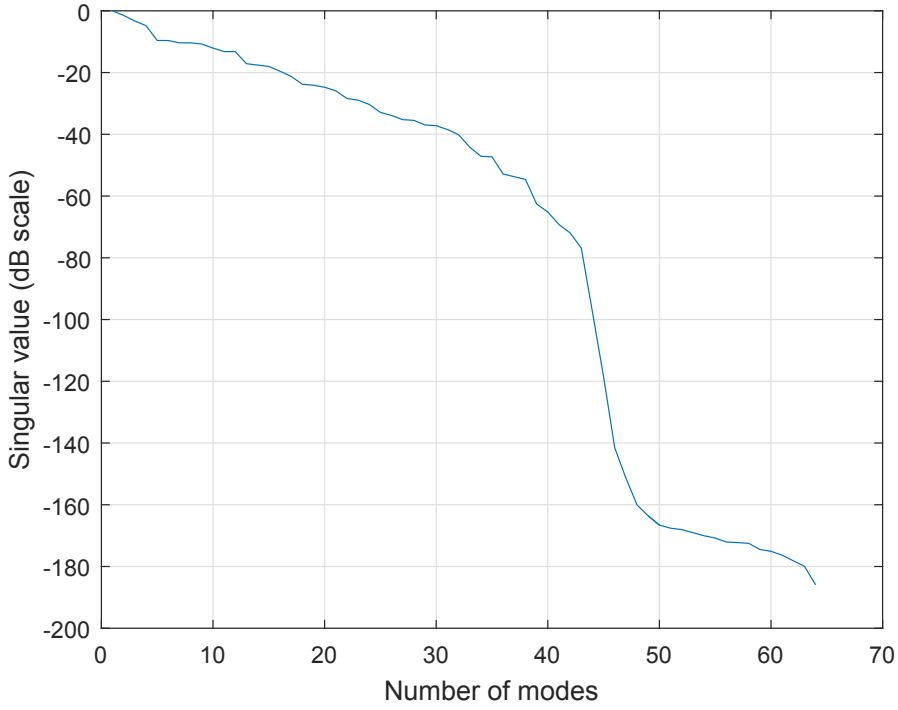

Figure 3: Singular values of the data matrix $\mathbf{X}$. Aluminium UXO shell, proud at 10m.

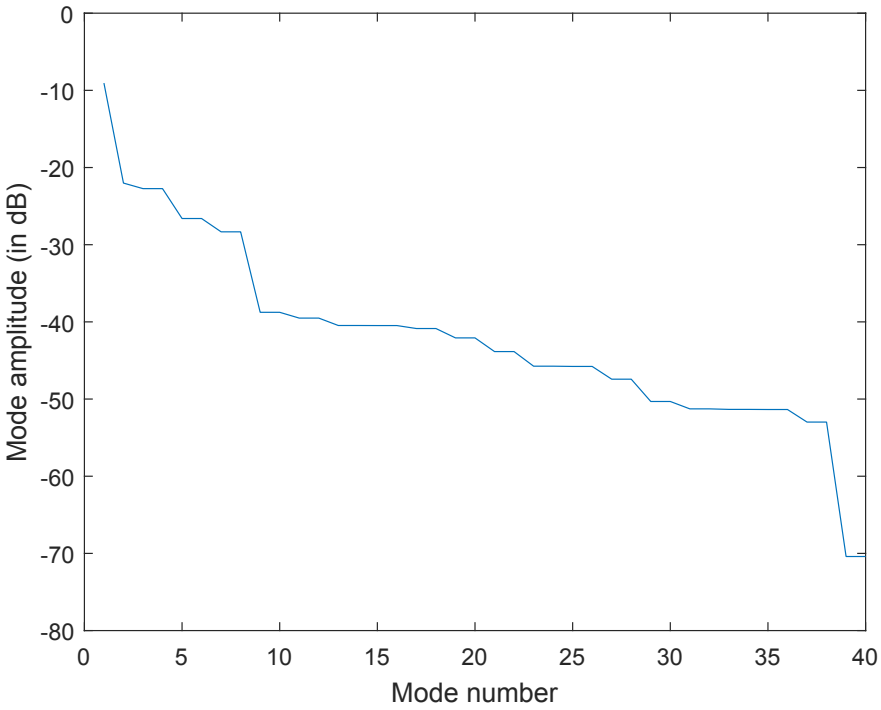

Figure 4: Mode amplitudes when using 40 modes ($M = 40$)

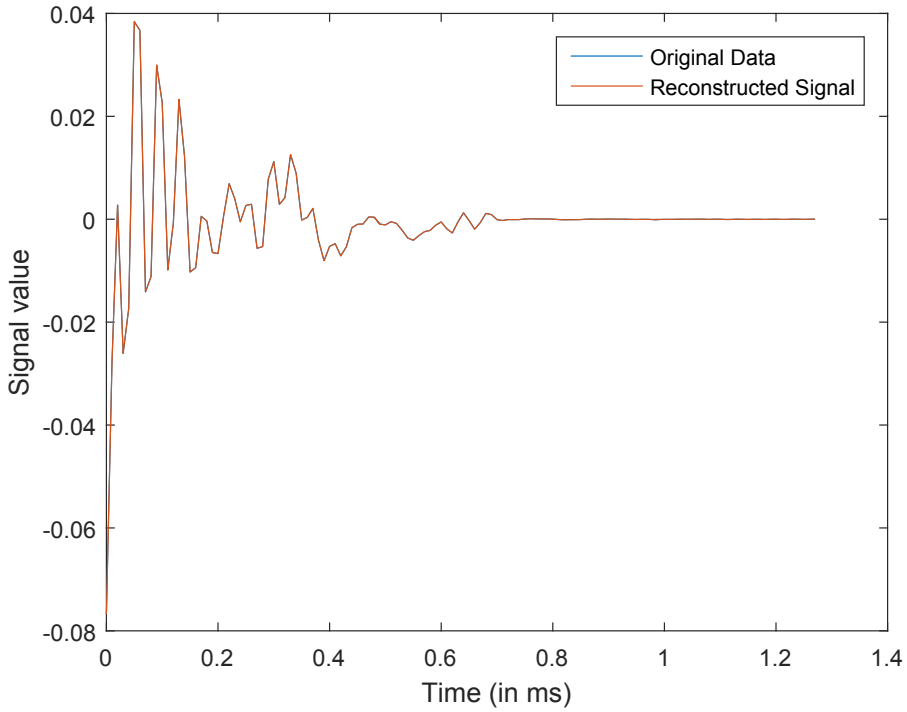

Figure 5: Original and reconstructed signal for $L = 63, M = 40$. Aluminium UXO shell, proud at 10m.

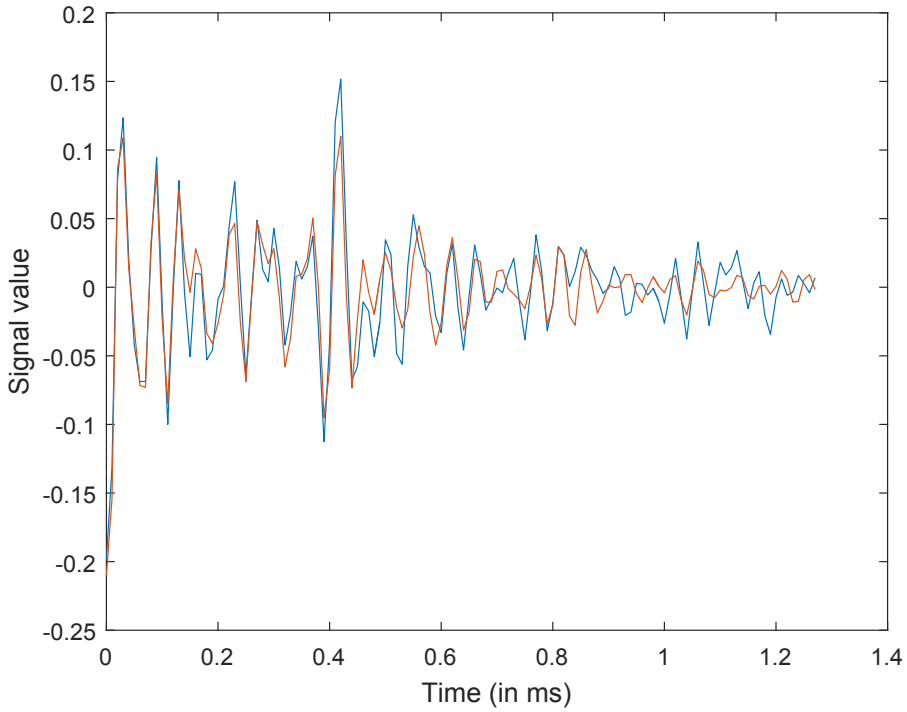

Figure 6: Original and reconstructed signal for $L = 63, M = 16$. Aluminium pipe.

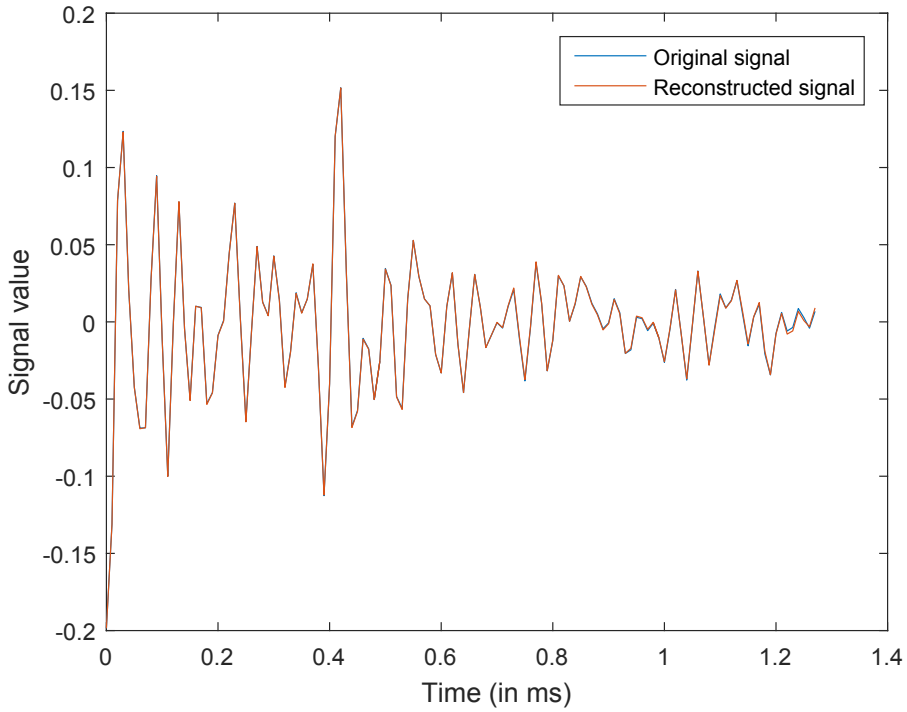

Figure 7: Original and reconstructed signal for $L = 63, M = 40$. Aluminium pipe.

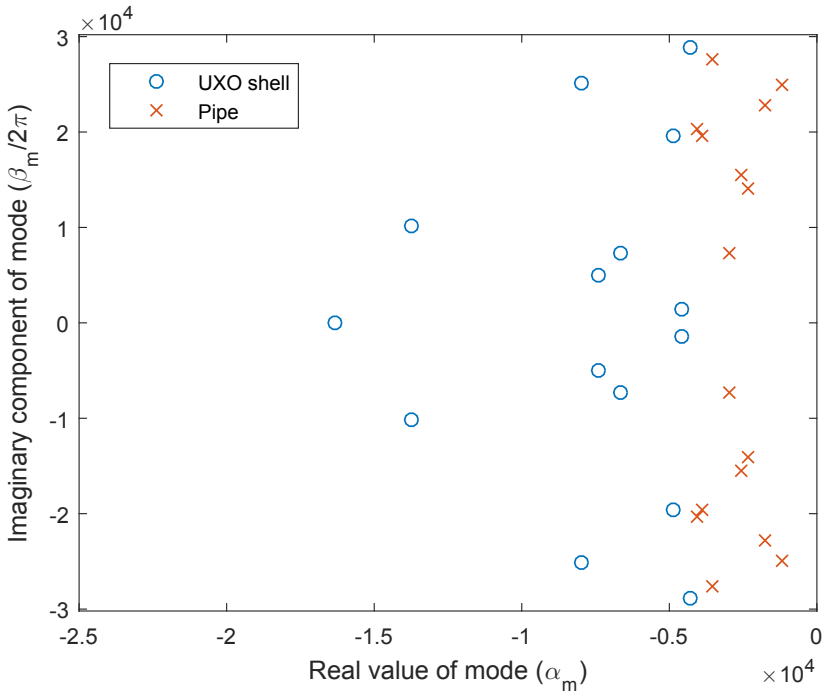

Figure 8: Comparing the modes for the aluminium pipe and UXO shell. $L = 63, M = 16$.

3.3 Comparing Targets Responses

As stated earlier, the motivation in using the Matrix Pencil approach is that it provides a simple way to estimate the fundamental modes of the object. In this section, we present the results of preliminary tests on a subset of targets within the PONDEX data sets. For purposes of visualization all results in this section use $M = 16$. Unless specified, the figures compare the complex modes obtained $(\alpha_m + j\beta_m)$. Specifically, to provide some physical intuition, we plot α_m - which we expect to be all negative since we have extracted the waning portion of the signal - and $\beta_m/2\pi$ which should have the dimensions of frequency. Since the excitation is restricted to 30 kHz, we expect these frequencies to be limited to ± 30 kHz.

Comparing Aluminium Pipe and UXO Shell Proud at 10m: The first comparison is between the aluminium pipe and the aluminium UXO shell, proud at 10m. These signals were plotted in Figs. 5 and 7. Comparing Figs. 5 and 7 clearly indicates that the aluminium pipe displays characteristics of ringing, i.e., the signal transient is far longer than for the UXO shell. This should, in turn, imply that the attenuation coefficients (α_m) for the pipe be smaller than for the UXO shell.

Figure 8 plots the 16 modes for each of the two targets obtained using the Matrix Pencil approach. The plot clearly shows that the attenuation factors for the pipe are significantly smaller than that for the UXO shell. This is consistent with our interpretation of Figs. 5 and 7.

Comparing UXO Shell Proud at 10m and at 5m: Figure 8 suggests that the Matrix Pencil method *does have the capability to distinguish between different kinds of targets.* In cases of significantly different targets, the modes extracted occupy two distinct regions in the complex plane. In this example, we compare the modes extracted for the same target measured at two different ranges: the aluminium UXO shell proud at 10m and at 5m.

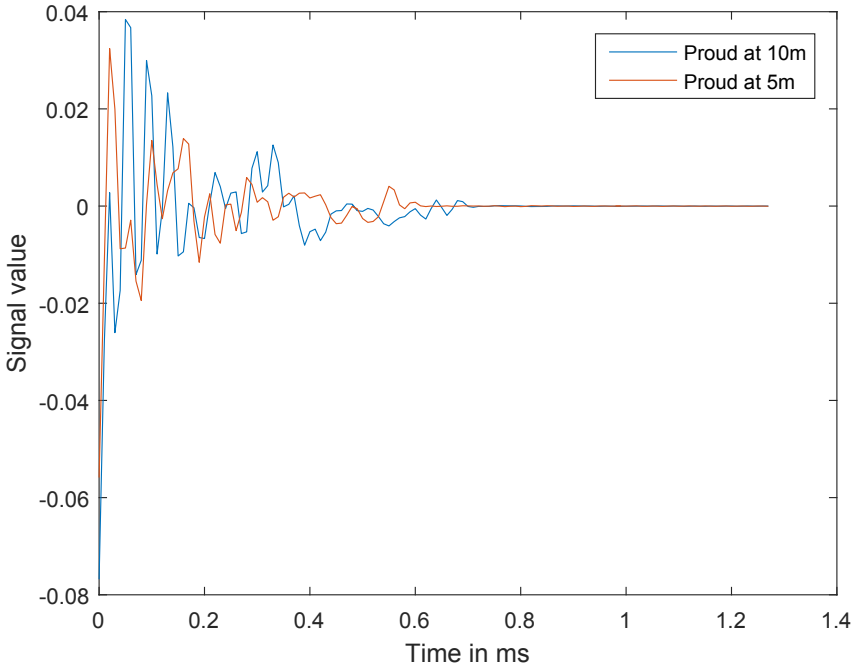

Figure 9: Measured signal for the UXO shell proud at 10m and at 5m.

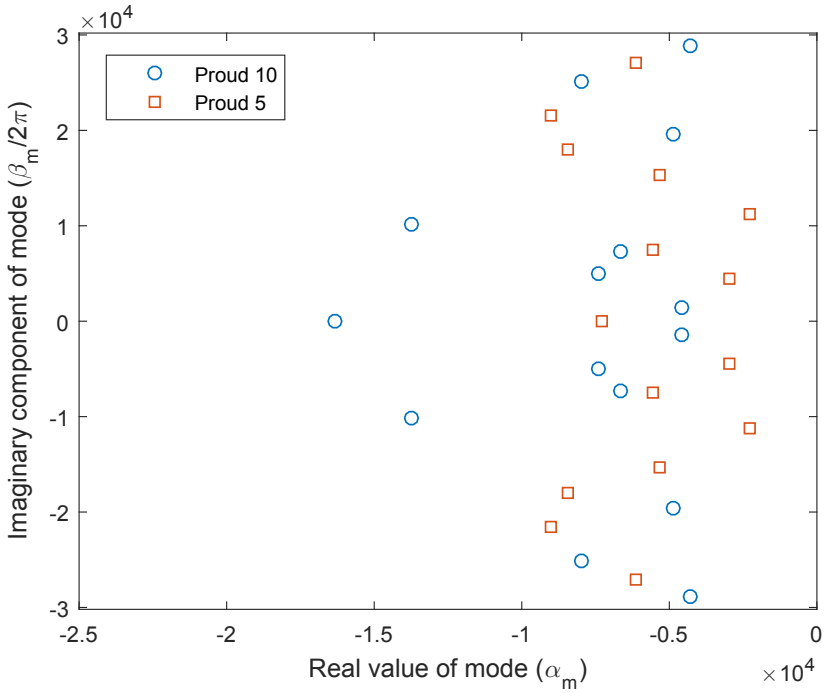

Figure 10: Modes extracted for the UXO shell proud at 10m and at 5m. $L = 63, M = 16$.

Figure 9 plots the pre-processed measured signals for the same target at the two ranges. The figure shows a surprisingly large differences between the two measured signals. For example, the signal for a range of 10m seems to die out faster at a range of 5m. It is not clear to us at this stage

why this should be the case. Given the large difference between the signals, it is not, therefore, surprising that the modes extracted are quite different as well. Figure 10 plots the extracted modes for the two cases. The lower attenuation of the signal at 5m range is clear, though there is a large overlap between the modes. However, worryingly, there is no discernible pattern to the mode distributions. In Fig. 8 it was immediately clear that the two sets of modes corresponded to different objects; in Fig. 10 it is not clear that the two sets of modes correspond to the same object.

Comparing UXO Shell Proud at 10m and Buried at 5m: Another comparison between the two measurements of the aluminium UXO shell is when the shell is buried at 5m and proud at 10m.

Figures 11 and 12 recreate Figs. 9 and 10 for this new comparison. Again, both the signals and the modes extracted are substantially different. On the other hand, there is a clearer structure to the modes - when the target is buried, the modes seem to separate out into two groups, one with a low attenuation factor and one with a higher attenuation factor.

Figures 10 and 12 taken together are cause for concern. The same target in different scenarios seems to yield different sets of modes. Absent a physical justification of why the reflected signals should be so different, these figures are cautionary. However, we do emphasize that these are preliminary results and warrant further investigation[1].

Comparing UXO Shell Proud at 10m and a Real Shell at 10m: Our final result compares two different targets again: the aluminium UXO shell proud (at 10m) and a real shell also at 10m. Figure 13 plots the two sets of modes for these two cases. As is clear, again, in comparing two *different* targets, the two sets of modes form two distinct groups and target discrimination may be possible.

4 Discussion

This report has detailed our preliminary investigation into the use of a model-based parameter estimation technique in target discrimination. Specifically, we use the Matrix Pencil approach to extract the characteristic modes of the measured target(s). The goal is to use these modes to form a detection metric. The results presented here are both promising and cautionary. In comparing the modes extracted by the Matrix Pencil approach for two different kinds of targets, there is a clear separation between the modes. This is evident in Fig. 8 (aluminium pipe and UXO shell) and in Fig. 13 (UXO shell and real shell). The separation is especially clear in the attenuation factor $(\alpha_m, m = 1, \ldots, M)$.

The cautionary results arose when we compared the modes extracted for the same target in different positions with respect to the sonar - one comparison had the UXO shell at two different ranges and the other compared the cases of the UXO shell proud at 10m and buried. Figures 9 and 11 showed that there are significant differences in the received signal, which translates to differences in the modes as well (Figs. 10 and 12). It is important to note, however, that the differences here appear to be smaller than in Figs. 8 and 13.

There are several more steps to be taken before any definitive conclusions can be drawn. The results in this report are based on a very specific pre-processing step wherein only the waning part of the signal (from its max absolute value forward) is taken into consideration. Further, a fixed

[1]Dr. John Fawcett, of DRDC, suggests a *possible* explanation: that the four paths (direct, two single-bounce and the one double-bounce) add up differently for the two ranges. If the frequency components get reflected and propagate differently, this could explain the signal differences seen, which, in turn, is reflected in the modes. One possible solution would be focus on cases where the target is as far from the sonar as possible.

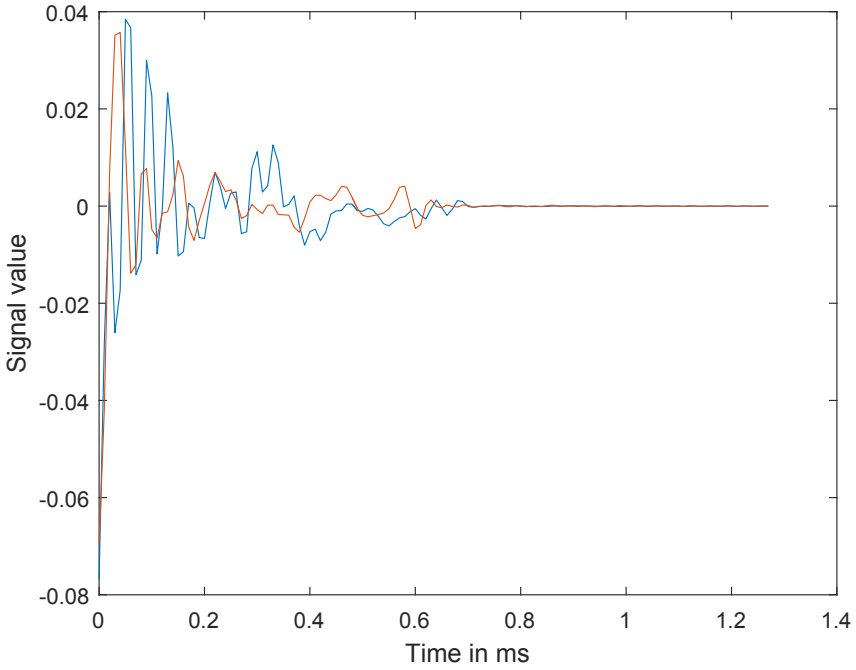

Figure 11: Measured signal for the UXO shell proud at 10m and buried at 5m.

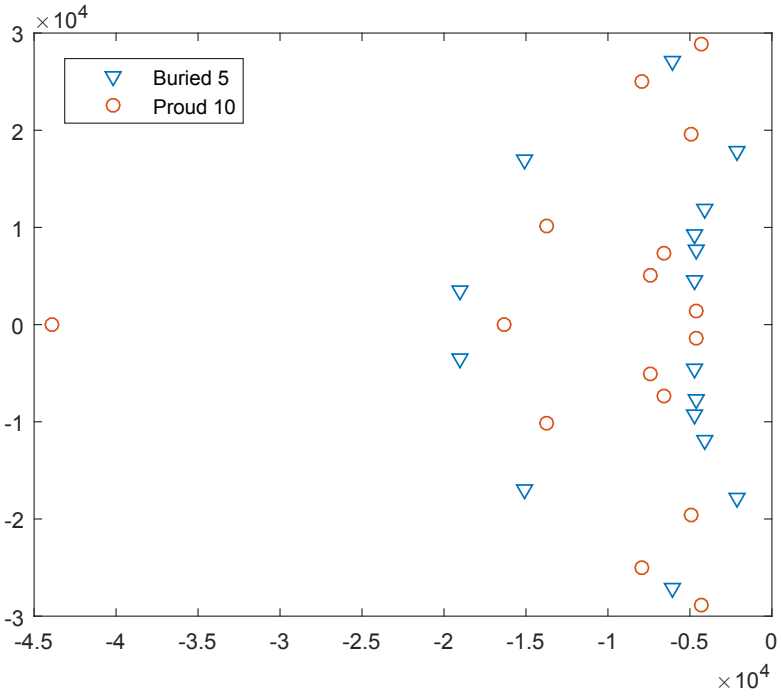

Figure 12: Modes extracted for the UXO shell proud at 10m and buried at 5m. $L = 63, M = 16$.

length of 128 samples is used. In this regard, at least half the signal is "thrown out"; including both the waxing and waning parts of the signal may provide better discrimination.

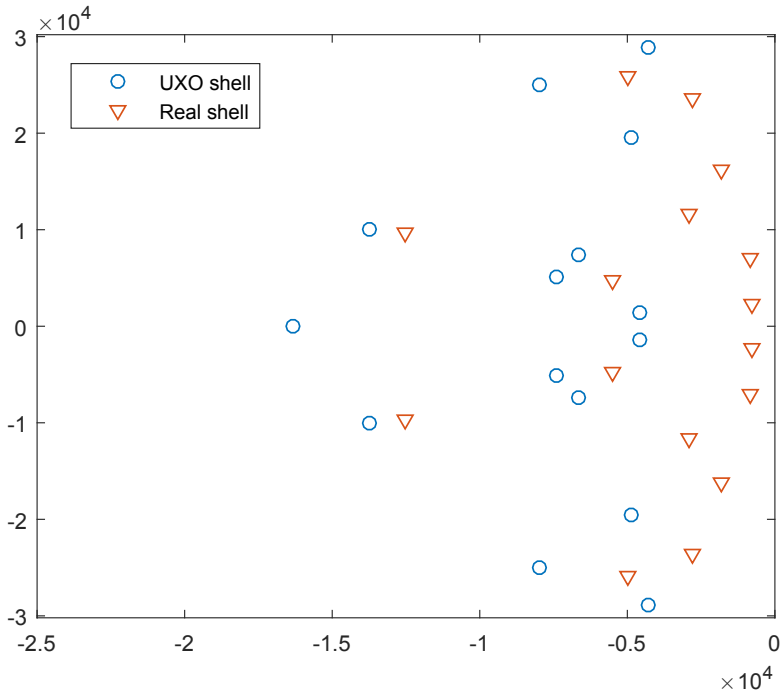

Figure 13: Modes extracted for the UXO shell proud at 10m and a real shell also at 10m. $L = 63, M = 16$.

Another (potentially) important consideration is that, so far, we have used signals "as is". However, the model in Eqn. (1) is most valid for the impulse response of the target, not the measured signal. One potential improvement, therefore, is to perform a deconvolution and remove the impact of the incident signal.

Finally, most comparisons here use either $M = 16$ or $M = 40$. There is no reason for the number of modes used be the same for different targets. Finally, any differences measured between two sets of modes must, somehow, account for the amplitudes of the modes. As we have seen (Fig. 4 for example), the estimated amplitudes of the individual modes show a wide dynamic range. Using an adaptive approach to estimating the number of modes, using for example the work in [8] may help. Furthermore, as mentioned earlier, it is not clear (yet) as whether it is the modes with the small amplitudes that provide the discrimination or the larger amplitude modes - or a weighted mix of all modes.

In summary, the first phase of this project is on track - the initial results are promising, but need further investigation before any definitive statements can be made.

References

[1] R. S. Adve, "Ultrawideband (UWB) high-resolution noise radar for concealed weapon detection," Tech. Rep. to DRDC Ottawa for Contract CDA 2008-C111-0046, January 2011, progress report.

[2] Y. Hua and T. K. Sarkar, "Matrix pencil method for estimating parameters of exponentially damped/undamped sinusoids in noise," *IEEE Transactions on Acoustics, Speech and Signal Processing*, vol. 38, pp. 814–824, May 1990.

[3] R. S. Adve, O. M. Pereira-Filho, T. K. Sarkar, and S. M. Rao, "Extrapolation of time domain responses from three dimensional objects utilizing the matrix pencil technique," *IEEE Transactions on Antennas and Propagation*, vol. 45, pp. 147–156, January 1997.

[4] R. S. Adve, T. K. Sarkar, S. M. Rao, E. K. Miller, and D. R. Pflug, "Application of the Cauchy method for extrapolating/interpolating narrowband system responses," *IEEE Transactions on Microwave Theory and Techniques*, vol. 45, Part 2, no. 5, pp. 837–845, May 1997.

[5] K. Bayat and R. S. Adve, "Joint toa/doa wireless position location using matrix pencil," in *Vehicular Technology Conference, 2004. VTC2004-Fall. 2004 IEEE 60th*, vol. 5, Sept 2004, pp. 3535–3539 Vol. 5.

[6] C. K. E. Lau, R. S. Adve, and T. K. Sarkar, "Minimum norm mutual coupling compensation with applications in direction of arrival estimation," *IEEE Transactions on Antennas and Propagation*, vol. 52, no. 8, pp. 2034–2041, Aug 2004.

[7] K. L. Williams, S. G. Kargl, E. I. Thorsos, D. S. Burnett, J. L. Lopes, and M. Z. abd P. L. Marston, "Acoustic scattering from an aluminum cylinder in contact with a sand sediment: Measurements, modeling, and interpretation," *Journal of Acoustics Society of America*, vol. 127, pp. 3356–3371, 2010.

[8] M. Wax and T. Kailath, "Detection of signals by information theoretic criteria," *IEEE Transactions on Acoustics, Speech and Signal Processing*, vol. 33, no. 2, pp. 387–392, April 1985.